

# Complete response characterization of ultrafast linear photonic devices

Tobias Kampfrath,<sup>1,\*</sup> Daryl M. Beggs,<sup>2</sup> Thomas F. Krauss,<sup>2</sup> and L. (Kobus) Kuipers<sup>1</sup>

<sup>1</sup>FOM Institute for Atomic and Molecular Physics (AMOLF), Science Park 104,  
1098 XG Amsterdam, The Netherlands

<sup>2</sup>School of Physics and Astronomy, University of St. Andrews, St. Andrews, Fife, KY16 9SS, UK

\*Corresponding author: kampfrath@amolf.nl

Received July 20, 2009; revised September 16, 2009; accepted September 18, 2009;  
posted October 8, 2009 (Doc. ID 114545); published October 29, 2009

We present a method to fully characterize linear photonic devices that change their properties on ultrashort time scales. When we feed the device with a broadband input pulse and detect the resulting output field for a sufficient number of arrival times of the input, the device response to any other input with smaller bandwidth can be extracted numerically, without the need for additional measurements. Our approach is based on the formalism of linear time-varying systems, and we experimentally demonstrate its feasibility for the example of an ultrafast nanophotonic switch. © 2009 Optical Society of America  
OCIS codes: 320.7080, 300.6530.

Optical devices can often be pictured as in the black-box scheme of Fig. 1, where an input light field  $E_i(t)$  results in the output light field  $E_o(t)$ , with  $t$  denoting time. Nowadays, ultrasmall devices with a tailored linear relationship between input and output can be fabricated by controlling the geometry of photonic materials on the nanometer scale. Examples are cavities [1–4], photonic crystals [5,6], and photonic-crystal waveguides [7,8]. The optical properties of these structures can be altered on a femtosecond time scale by illumination with an intense pump laser pulse, as indicated in Fig. 1 [1–7]. To obtain the output of such a linear time-varying system to any input pulse, it is highly desirable to have a method that fully characterizes the device by measuring its response to just one type of input. In this context, previous work has focused on rather special systems with negligible time or wavelength dependence [9–12].

In this Letter, we use the transfer-function formalism to show that a linear time-varying device is fully characterized by measuring its output field over a wide range of arrival times of a broadband input pulse. In particular, the response to any input with smaller bandwidth can then be extracted numerically, without the need for additional measurements. We experimentally demonstrate the strength of this approach for an ultrafast nanophotonic switch. We believe that our method is highly suited for a full and time-effective characterization of ultrafast linear photonic devices [1–7].

When the input power of the device of Fig. 1 is sufficiently low, the relationship between the input and output fields is linear and in its most general form is given by the generalized convolution [13]

$$E_o(t) = \int dt' \mathcal{T}(t, t') E_i(t'). \quad (1)$$

Equation (1) shows that the output at time  $t$  is determined by the history  $E_i(t')$  of the probing input. The so-called transfer function  $\mathcal{T}(t, t')$  depends on two

time parameters and can be interpreted as the response to a  $\delta$ -like input centered at time  $t'$ . Since a linear system is fully characterized by its transfer function, it is highly desirable to measure  $\mathcal{T}$ . So far, measurement schemes have been realized for linear time-invariant (LTI) [9] and linear frequency-invariant (LFI) [10–12] photonic devices, where a one-dimensional data set is sufficient. LTI devices do not change their properties in the course of time and fulfill  $\mathcal{T}(t, t') = \mathcal{T}(t - t', 0)$  [13]. Then, Eq. (1) reduces to the familiar relationship  $\mathcal{F}E_o(\omega) = \mathcal{F}_1 \mathcal{T}(\omega, 0) \mathcal{F}E_i(\omega)$ , where  $\mathcal{F}$  denotes the Fourier transformation [14] and  $\omega$  is the angular frequency.  $\mathcal{F}_j f$  is the Fourier transformation of  $f$  with respect to the  $j$ th argument of  $f$ . LFI devices, on the other hand, do not exhibit any wavelength dependence and have a transfer function  $\mathcal{T}(t, t') = a(t) \delta(t - t')$ , where  $a(t)$  is an arbitrary function of  $t$  [13].

The two-time method introduced here requires neither the LTI nor the LFI constraints and applies to the general case where the device properties are both time and wavelength dependent. In essence, we create a two-dimensional data set  $E_o(t, \tau)$  by measuring the device output for various delay times  $\tau$  between a

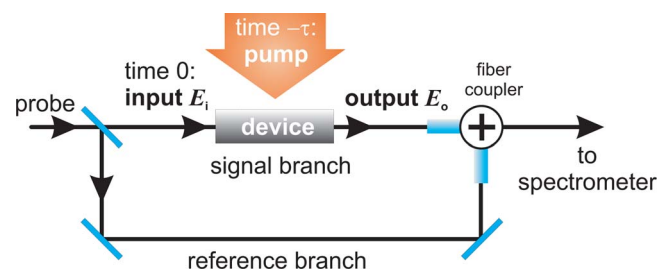


Fig. 1. (Color online) Schematic of an abstract black-box system that produces an output signal  $E_o$  as a response to an input signal  $E_i$ . An external stimulus like an intense pump laser pulse arriving at time  $-\tau$  makes the optical properties of the device time dependent. In the characterization experiment, a broadband probe pulse  $E_i$  enters the device at time 0, and the resulting output field  $E_o$  is detected via interference with a reference pulse.

probing broadband input and the actuating pump pulse. As indicated in Fig. 1, the input pulse arrives at the device at time 0 and the pump pulse at time  $-\tau$ . According to Eq. (1), the output electric field is then  $E_o(t, \tau) = \int dt' \mathcal{T}(t + \tau, t' + \tau) E_i(t')$ . Remarkably, after a double Fourier transformation  $\mathcal{F}_{12} = \mathcal{F}_1 \mathcal{F}_2$  of  $E_o$ , this equation turns into the factorized relationship  $\mathcal{F}_{12} E_o(\omega, \Omega) = \mathcal{F}_{12} \mathcal{T}(\omega, \Omega - \omega) \mathcal{F} E_i(\omega - \Omega)$ . As we aim to determine the device response  $E'_o$  to any other input  $E'_i$ , we apply the last equation to  $E'_i$  as well and obtain

$$\mathcal{F}_{12} E'_o(\omega, \Omega) = \mathcal{F}_{12} E_o(\omega, \Omega) \frac{\mathcal{F} E'_i(\omega - \Omega)}{\mathcal{F} E_i(\omega - \Omega)}, \quad (2)$$

which is the central result of this section. As suggested by Eq. (2), the spectrum of  $E'_i$  should be narrower than that of the reference input  $E_i$  to avoid noise problems. We now put Eq. (2) to the test and measure the output of an ultrafast nanophotonic switch as a function of  $\tau$  for both a broadband and a narrowband input pulse. The narrowband output *extracted* via Eq. (2) can then be directly compared to the narrowband output *measured*.

Figure 1 shows a schematic of our experimental setup. Laser pulses with an energy of 25 nJ, a duration of 100 fs FWHM of the intensity (FWHMI), a center wavelength of 810 nm, and a repetition rate of 80 MHz from a Ti:sapphire laser oscillator pump an optical parametric oscillator to generate 180 fs, 1482 nm pulses. The spectrum of these pulses can be optionally narrowed using a single-grating-based reflective pulse shaper [15]. The obtained bandwidth-limited pulses  $E_i$  are fed into the sample device, and the resulting output  $E_o$  is picked up by a lensed fiber. Since Eq. (2) requires knowledge of the electric field of the broadband output, we use a small part of the input beam as a reference and let it interfere with the output pulse by means of a fiber coupler, as seen in Fig. 1. By measuring the intensity spectra of the reference pulse, the device output pulse, and the sum of both pulses with an optical spectrum analyzer, we are able to retrieve the output electric field  $\mathcal{F}_1 E_o(\omega, \tau)$  [16]. Crucial experimental prerequisites of such broadband spectral interferometry are a well-defined input pulse, dispersion-balanced sample and reference paths, and a low probe power to avoid nonlinear effects. In addition, the signal and reference paths have to remain stable on a subwavelength level over the  $\sim 20$  min duration of the experiment.

The device under investigation is a nanophotonic switch with a footprint of  $10 \mu\text{m} \times 10 \mu\text{m}$  based on two coupled waveguides in a periodically perforated Si photonic-crystal membrane. Details on principle and fabrication can be found in [7,8]. To actuate the switch, about 2% of the output of the Ti:sapphire oscillator is used to pump the entire switch from above, as indicated by Fig. 1. Each pump pulse generates electron-hole pairs with a density of the order of  $1 \times 10^{18} \text{ cm}^{-3}$  in the Si membrane, which induces a sudden drop of the Si refractive index and so triggers the switch [7].

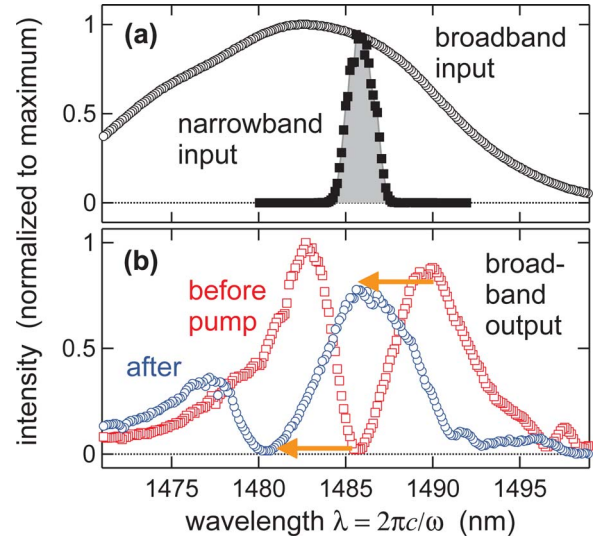


Fig. 2. (Color online) (a) Intensity spectra of the 180 fs broadband and 1.9 ps narrowband input pulse  $E_i$  and  $E'_i$ , respectively, used in this work. (b) Output spectra  $|\mathcal{F}_1 E_o(\omega, \tau)|^2$  resulting from the broadband input of (a) at 10 ps before and after arrival of the pump pulse, respectively.

Figure 2(a) shows the spectral intensity of the 180 fs broadband and the 1.9 ps FWHMI narrowband input pulse as a function of the wavelength  $\lambda = 2\pi c/\omega$ . The broadband input results in the output spectra of Fig. 2(b) that are obtained 10 ps before and after arrival of the pump pulse. As indicated by the arrows in Fig. 2(b), the absorption of the pump pulse mainly induces an ultrafast blueshift of the instantaneous transmittance spectrum of the switch [7]. This behavior becomes even more evident in the color plot of Fig. 3(a), which displays the broadband output spectra  $|\mathcal{F}_1 E_o(\omega, \tau)|^2$  as a function of the pump-probe delay  $\tau$ . Note how the various minima and maxima

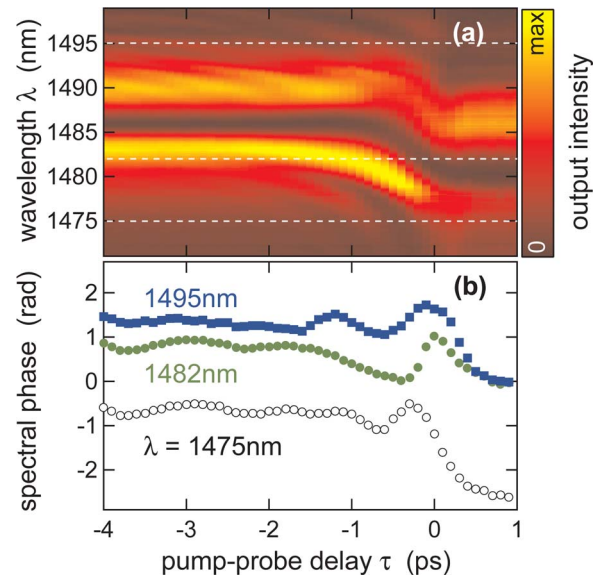


Fig. 3. (Color online) (a) Intensity spectra of the output pulses resulting from the broadband input of Fig. 2(a) as a function of the pump-probe delay  $\tau$ . (b) Phase of  $\mathcal{F}_1 E_o(\omega, \tau)$  for selected wavelengths marked as dashed lines in (a).

shift by about 5 nm to lower wavelengths in the vicinity of  $\tau=0$ . The measured phase information is displayed in Fig. 3(b) for three example wavelengths, and the temporal changes in  $\arg \mathcal{F}_1 E_o(\omega, \tau)$  are clearly correlated with the amplitude changes of Fig. 3(a).

As Fig. 3 represents the full information on the output field  $E_o$ , we can employ Eq. (2) to calculate the device output  $E'_o$  for any input  $E'_i$ , and we choose here the 1.9 ps narrowband input of Fig. 2(a). As seen in Fig. 2(b), the spectrum of  $E'_i$  lies in a minimum of the broadband output before the arrival of the pump pulse and in a maximum after. Therefore, a distinct switch-on of the device output for this input is expected. We use the discrete Fourier transformation to calculate  $\mathcal{F}_{12} E_o(\omega, \Omega)$  from  $\mathcal{F}_1 E_o(\omega, \tau)$ . To increase the  $\Omega$  resolution, we extend the data of Fig. 3 by a constant continuation from  $\tau=-4$  ps to  $-50$  ps and from  $\tau=1$  ps to  $50$  ps. This procedure is justified since the pump-induced change in the Si refractive index decays on a much slower time scale of about 0.4 ns [7]. The Fourier amplitudes  $\mathcal{F} E_i(\omega-\Omega)$  and  $\mathcal{F} E'_i(\omega-\Omega)$  of the bandwidth-limited input pulses are obtained by linear interpolation of the square root of the measured input spectra of Fig. 2(a).

Figure 4(a) shows the resulting narrowband output spectra of the device as a function of the pump-arrival time  $\tau$ . As expected, the output is initially dark but then suddenly flashes up around  $\tau=0$ . We now compare these *extracted* data to Fig. 4(b), which displays the output *measured* for the same narrowband input. The agreement between Figs. 4(a) and 4(b) is excellent, even for the fine structures at  $\tau < 0$ . These results verify that our approach based on Eq. (2) and the setup of Fig. 1 is indeed feasible for the broadband characterization of ultrafast photonic devices.

While Eq. (2) applies to all square-integrable signals, the interferometric frequency-domain detection used here imposes practical constraints. First, the

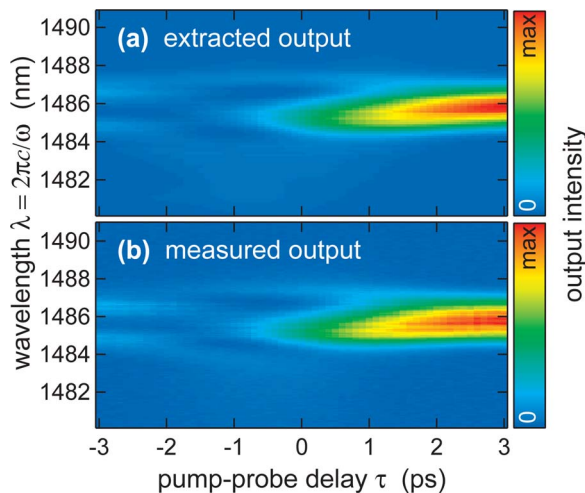


Fig. 4. (Color online) (a) Device response to the narrowband input pulse shown in Fig. 2(a) as extracted from the data in Figs. 2(a) and 3 by virtue of Eq. (2). (b) Device output measured. Note the excellent agreement of both figures.

spectral resolution of the spectrometer has to be smaller than the inverse duration of the output signal in the  $t$  domain. Second, our interferometer yields a signal  $(\mathcal{F} E_r)^*(\omega) \mathcal{F}_1 E_o(\omega, \tau)$  [16], where the reference pulse  $E_r$  is a copy of the input pulse. Equation (2) then implies that the narrowband output  $E'_o$  can be determined only for frequencies  $\omega$  at which  $\mathcal{F} E_r$  is well above the noise level. This condition does not pose a restriction for the data considered here, as the narrowband output [Fig. 4(b)] is fully covered by the spectrum of the broadband input [Fig. 2(a)]. In case the sample changes so fast that new components with frequencies  $\omega-\Omega$  outside the spectrum of  $E_r$  are generated, a more broadband reference or nonlinear schemes [17] should be used to detect  $E_o$ .

We thank Katrin Domke for advice and acknowledge funding through the EU FP6-FET “SPLASH” project. This work is part of the research program of the Stichting voor Fundamenteel Onderzoek der Materie (FOM), which is supported by the Nederlandse Organisatie voor Wetenschappelijk Onderzoek (NOW).

## References and Notes

1. S. F. Preble, Q. Xu, and M. Lipson, *Nat. Photonics* **1**, 293 (2007).
2. P. J. Harding, T. G. Euser, Y.-R. Nowicki-Bringuier, J.-M. Gérard, and W. L. Vos, *Appl. Phys. Lett.* **91**, 111103 (2007).
3. X. Hu, P. Jiang, C. Ding, H. Yang, and Q. Gong, *Nat. Photonics* **2**, 185 (2008).
4. M. Waldow, T. Plötzing, M. Gottheil, M. Först, J. Bolten, T. Wahlbrink, and H. Kurz, *Opt. Express* **16**, 7693 (2008).
5. S. W. Leonard, H. M. van Driel, J. Schilling, and R. B. Wehrspohn, *Phys. Rev. B* **66**, 161102 (2002).
6. D. A. Mazurenko, R. Kerst, J. I. Dijkhuis, A. V. Akimov, V. G. Golubev, A. A. Kaplyanskii, D. A. Kurdyukov, and A. B. Pevtsov, *Appl. Phys. Lett.* **86**, 041114 (2005).
7. T. Kampfrath, D. M. Beggs, T. P. White, M. Burreli, D. van Oosten, T. F. Krauss, and L. Kuipers, *Appl. Phys. Lett.* **94**, 241119 (2009).
8. D. M. Beggs, T. P. White, L. O’Faolain, and T. F. Krauss, *Opt. Lett.* **33**, 147 (2008).
9. A. Gomez-Iglesias, D. O’Brien, L. O’Faolain, A. Miller, and T. F. Krauss, *Appl. Phys. Lett.* **90**, 261107 (2007).
10. C. Dorrer and I. Kang, *Opt. Lett.* **27**, 1315 (2002).
11. F. P. Romstad, D. Birkedal, J. Mørk, and J. M. Hvam, *IEEE Photon. Technol. Lett.* **14**, 621 (2002).
12. Y. Park, T.-J. Ahn, and J. Azaña, *Opt. Express* **17**, 1734 (2009).
13. M. C. Jeruchim, P. Balaban, and K. S. Shanmugan, *Simulation of Communication Systems: Modeling, Methodology and Techniques* (Kluwer, 2000).
14. In this work, the Fourier transform and its inverse are defined by  $\mathcal{F}f(\omega) = \int dt f(t) \exp(i\omega t)$  and  $f(t) = \int d\omega \mathcal{F}f(\omega) \exp(-i\omega t) / 2\pi$ , respectively.
15. R. D. Nelson, D. E. Leaird, and A. M. Weiner, *Opt. Express* **11**, 1763 (2003).
16. L. Lepetit, G. Chériaux, and M. Joffre, *J. Opt. Soc. Am. B* **12**, 2467 (1995).
17. R. Trebino, *Frequency-Resolved Optical Gating: the Measurement of Ultrashort Laser Pulses* (Kluwer, 2002).